

## Reliable modeling of discharge process for adsorbed natural gas storage tanks

Mahdi Khorashadizadeh\*, Mahdi Niknam Shahrak\*\*, and Akbar Shahsavand\*<sup>†</sup>

\*Chemical Engineering Department, Faculty of Engineering Ferdowsi University of Mashhad, Mashhad, P. O. Box 91775-1111, Iran

\*\*Department of Chemical Engineering, Quchan University of Advanced Technology, Quchan, P. O. Box 84686-94717, Iran

(Received 16 July 2013 • accepted 8 April 2014)

**Abstract**—Natural gas consumption has doubled in the last fifteen years. Among all storage techniques, adsorbed natural gas (ANG) provides a reliable vehicle for safe utilization of natural gas. Despite all favorable characteristics of the ANG process, thermal adverse effects during charge and discharge processes are the most challenging issues facing adsorbed natural gas applications, especially for automotive usage. Mathematical modeling of an ANG tank can provide a reliable method to analyze and solve such problems. A robust and lumped model is presented to mimic the discharge process of an ANG tank storing pure component. The proposed model is very convenient compared to other available conventional models that require extensive computational efforts. Two experimental measurements and two simulation data sets (borrowed from literature) are recruited to validate the model predictions. The simulation results indicate proper agreement between the proposed model predictions and the validation data.

Keywords: Natural Gas Storage, Adsorption, ANG, Lumped Modeling, Discharge Process

### INTRODUCTION

Availability, clean burning and low price are some of the most important reasons to focus researches on using natural gas (NG) in various industries such as automotive industry in the last two decades [1-28]. Despite the benefits of NG, its storage, transportation, and energy density are the most serious problem in the way of spread of its application. Several storage techniques are developed to cope with this issue. Compressed natural gas (CNG) storage technique is presently the most popular method to use natural gas in on-board reservoirs for automotive applications. However, it suffers from a number of shortcomings: extremely high pressure requirement (200-250 bar), high cost due to its high pressure, heavy vessels and restricted storage reservoir geometries.

LNG is another available method to store and transport natural gas. LNG provides highest energy density (around 600 volumes of natural gas per volume of the ANG vessel (v/v)) amongst other forms of natural gas storage techniques. But it cannot be easily and directly used in cars or other vehicles due to its extremely low temperature requirements ( $-163\text{ }^{\circ}\text{C}$ ) [17]. Moreover, use of LNG needs appropriate technical equipment, so it is necessary to find a cheaper and safer method to store natural gas for vehicle usage. In the same manner, natural gas hydrate (NGH) storage can also be used for long distance transportation of large quantities of natural gases [29,30].

Adsorbed natural gas, which has gained more attention in the last couple of decades, is a promising alternative to CNG, LNG and NGH. In this application, maximization of gas storage density is the ultimate requirement, in order to store and deliver highest volume of

gas per volume of ANG storage vessel (v/v). Depending on the adsorbent (confined in the vessel), the delivered v/v will be different and so will the energy density. In 2000, the U.S. Department of Energy (DOE) raised the material-based adsorbed methane storage target from 150 to 180 v/v at 298 K and 35 bar [18,23]. New materials are synthesized every day to increase the v/v amount of NG storage capacity. The overall performance and practicality of ANG vessels also depend on the characteristics of the adsorbent as well as the heat and mass properties of the system.

Although ANG does not have some of CNG, NGH and LNG problems and can be considered as the most promising way in on-board natural gas storage technique among other scenarios, there are some challenges. Thermal effects in the bed during charge and discharge processes are the major problems facing ANG applications. Since adsorption and desorption of stored gas in the vessel are exothermic and endothermic, respectively, the heat released or demanded in these processes reduces the storage capacity. Thus, a profound understanding of heat and mass transfer phenomena occurring in ANG tank during charge and discharge processes is essential for better design of such reservoirs. Several experiments have been carried out [14,16,19] to address the thermal behavior of ANG storage technique during charge and discharge processes. The real response of such processes can be analyzed and studied by resorting to a suitable mathematical model. A brief review of such attempts for lumped [3,21,25] and distributed [1,2,5,8,18,20,26,28] modeling of ANG storage vessels during charge and discharge processes is presented below.

In a comprehensive pioneering work in 1996, Chang and Talu [1] studied the impact of heat of adsorption on ANG performance during discharge process under realistic condition of a vehicle application. The effect of various parameters on the ANG performances such as flow direction, demand rate and outside condition was also

<sup>†</sup>To whom correspondence should be addressed.

E-mail: shahsavand@um.ac.ir

Copyright by The Korean Institute of Chemical Engineers.

investigated. They reported that: "Moderation of the temperature drop under any ambient condition was one of the most important performances which can be easily obtained by changing flow direction from axial to radial." Their model predictions were ultimately validated using experimental temperature measurement provided by themselves.

In early 1997s, Mota et al. [2] investigated theoretically and mathematically the effect of diffusional resistances on charge dynamics for a granular activated carbon. Their study was focused on thermal effects and hydrodynamics of natural gas flow through the carbon bed. They included an extra intra-particle transport in their computational model. The research suffered from a lack of validation section. In the same year, Zhou [3] used two simple models for slow depressurization of a high-pressure gas-filled vessel and discussed the inherent differences and similarities of these mathematical models and their solutions. He derived a formula specifying the minimum possible wall temperature from comprehensive investigation of the analytical solution of the direct mass discharge model. The effects of various parameters such as heat transfer on external and internal walls of ANG vessel, discharge rate and thermal capacity ratio between the wall and the contained fluid were also investigated.

In 2000, Vasiliev et al. [5] tested and analyzed a new micro-porous adsorbent (active carbon fiber disks, produced from pyrolysis of cellulose: Busofit) which was capable of delivering near 150 v/v methane at 3.5 MPa pressure. They introduced a distributed model to predict the temperature profile during the radial gas discharge inside a cylindrical ANG vessel. The vessel was equipped with internal finned heaters for thermal control purposes. An ANG vessel (containing seven cylinders) with total volume of 43 liters was used to gather the experimental desorption data. The model predictions on pressure, temperature and mass of methane histories were fairly in agreement with measured data.

In 2005, Bastos-Neto et al. [8] provided experimental data on ANG storage and its delivery on activated carbon for the pressures of up to 40 atm. They compared their experimental data with their proposed lumped model. Although the obtained results of their model were in good agreement with experimental data, their model did not precisely include the heat effects corresponding to variations of adsorption heat with respect to loading and changes in room temperature throughout the experiments.

In 2009, Hirata et al. [18] modeled and solved the slow discharge process of a methane tank filled with porous carbonaceous adsorptive material by resorting to generalized integral transform technique (GITT). They validated their predictions by comparing them with synthesized and experimental data borrowed from the literature [1,2]. In the same year, Santos et al. [20] presented a numerical study for a new tank configuration used to store natural gas via adsorption. They used a computational code, based on the finite-volume method, to solve the equations that describe the dynamics of the charge process.

In 2010, Da Silva and Sphaier [21] presented several dimensionless groups associated with the heat and mass transfer within ANG vessels for lumped formulation. They claimed that their proposed groups can be easily used for multi-dimensional modeling of ANG discharge process, ultimately concluding that the lumped analysis is valid for longer process times. Evidently, lumped formulations could not provide correct predictions for shorter discharge times,

because the main assumption behind lumped models is that spatial variations should be small.

In 2011, Rahman et al. [26] used a finned-tube heat exchanger placed inside a pressurized ANG cylinder. A distributed model was employed for the simulation of both charge and discharge processes. They concluded that both the charge and discharge processes are notably enhanced due to the insertion of the fins and tubes in the adsorbent bed. The simulation results were not validated by any real experimental data. In the same year, Diaz and Sphaier [28] presented a methodology for analysis of heat and mass transfer in ANG storage vessel via a set of physically meaningful dimensionless groups. They validated their proposed model using data points borrowed from Hirata et al. [18]. They reported that their dimensionless groups facilitate analysis and simulation.

In the most recent study, Jurumenha and Sphaier [25] investigated the suitability of a lumped-capacitance formulation to simulate adsorbed natural gas storage processes. They obtained the lumped model by averaging from a multidimensional formulation. Finally they used Biot and Fourier dimensionless groups to determine whether a lumped-capacitance model can be accurately employed or not. They concluded that disparities were larger for smaller values of the Fourier number and higher values of the Biot number, indicating that the lumped formulation should not be employed for fast processes or with a high convective heat transfer at the outer surface. Moreover, Fourier number had a more pronounced effect than the Biot number, such that for large Fourier numbers the Biot number has practically no effect on the disparity between the formulations.

In the present article, thermal behavior of an ANG storage compartment is modeled via a convenient lumped formulation. The porosity variation effect during desorption process on the overall performance of the model is considered, which was not addressed previously. The accuracy and superior performances of the proposed model were validated using two experimental measurements [1,16] and two simulation data sets [2,18].

## PROCESS DESCRIPTION

Since the experimental or simulation data, used in this work for validation purposes, are borrowed from various studies [1,2,16,18], the typical corresponding experimental setups used in those works will be briefly reviewed here. The majority of the experiments were performed with the ANG test system shown in Fig. 1. The apparatus consisted of two main parts: the control unit and the test cylinders [1]. The flow rate is controlled by flow control unit. Some ther-

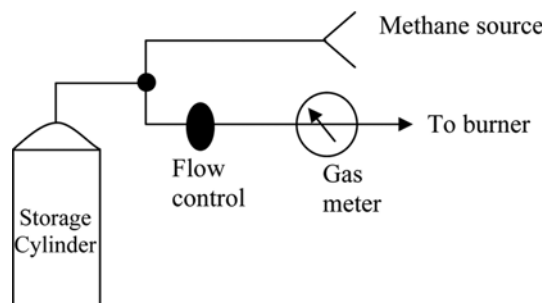


Fig. 1. Simple schematic of ANG storage system.

mocouples are installed on the cylinder to measure temperature inside the reservoir. In almost all ANG studies activated carbon has been the adsorbent material. The adsorption beds were considered a horizontal cylinder in the Mota et al. generated data [2] and a vertical cylinder in Chang and Talu and Ridha et al. experiments [1,16].

### MATHEMATICAL MODEL OF THE DISCHARGE PROCESS

The objective of this work is to present a convenient mathematical model for reliable estimation of transient temperature profiles during discharge of adsorbed natural gas from ANG storage vessels. The experimental and simulation data will be used to validate the performance of the proposed lumped model which is more convenient and provides reliable and robust predictions.

The gas adsorbed in the ANG vessel is considered to be a uniform mass with a spatially uniform temperature. The heat transfer between ANG vessel and the environment ( $T_\infty$ ) is assumed to be solely performed via free convection ( $h_\infty$ ). Other assumptions are: fixed discharge flow rate, negligible mass transfer resistance, Langmuir equilibrium adsorption, constant adsorbent physical properties, and Joule-Thomson coefficient.

With the above assumptions in mind, the overall lumped mass and energy balance equations for the discharge process can be written as:

$$\frac{d}{dt}(\varepsilon_{eff}C) + \frac{dq}{dt} = 0 - \frac{n_{out}}{V_b} \quad (1)$$

$$\frac{d}{dt} \left[ \left( \rho_g C_{pg} \varepsilon_{eff} + \rho_s C_{ps} (1 - \varepsilon_b) + C_{pl} \frac{qM_g}{1000} \right) T \right] = H_{ads} \frac{dq}{dt} + \frac{q_A}{V_b} - \frac{n_{out} H_{out}}{V_b} \quad (2)$$

where,  $C$  is gas phase concentration and it can be related to ANG vessel pressure and temperature via suitable equation of state ( $C=P/zRT$ ). The average value of 0.92 is computed for fluid compressibility factor using Peng-Robinson equation of state. Neglecting all mass transfer resistances, the adsorbed amount ( $q$ ) can be related to gas phase concentration (or its pressure) via proper isotherm such as Langmuir:

$$q = \frac{q_s b P}{1 + b P} \quad (3)$$

Temperature dependency of Langmuir parameters can be represented as [2]:

$$b = \beta e^{\gamma/T} \quad (4)$$

$$q_s = \theta T^\eta \quad (5)$$

All constant parameters ( $\beta$ ,  $\gamma$  and  $\eta$ ) are case dependent and should be specified correctly for the situation at hand.

The total porosity of adsorbent can be estimated from pore volume ( $V_p$ ), bulk density ( $\rho_b$ ), and bulk porosity  $\varepsilon_b$  as ( $\varepsilon_t = V_p \rho_b + \varepsilon_b$ )<sup>\*</sup>. The following equation considers the variations of effective porosity due to the reduction of adsorbed amount ( $q$ ) during the discharge process.

$$\varepsilon_{eff} = \varepsilon_t - \frac{q \cdot M}{1000 \rho_l} \quad (6)$$

The left hand side terms of mass balance Eq. (1) represent accumulation in gas and solid phases, while the terms on the right-hand side show input and output flow rates, respectively. Similarly, all the left-hand side terms of energy balance equation provide the energy accumulation in gas, solid and adsorbed phases. The right-hand side terms of Eq. (2) represent heat of desorption (heat sink), heat transfer with the environment ( $q_A = hA(T - T_\infty)$ ) and the enthalpy of discharged gas which has constant volumetric flow rate ( $Q_g$ ). Simultaneous solution of Eqs. (1) to (3) can provide the time distributions of  $P$ ,  $q$ , and  $T$ .

To achieve this goal, a relation should be found between the vessel temperature and the discharged gas temperature after throttling valve. For a known exit pressure ( $P_v$ ), the temperature of the gas leaving the valve ( $T_v$ ) can be evaluated using Joule-Thomson coefficient:

$$\mu = \frac{dP}{dT} = \frac{P - P_v}{T - T_v} \rightarrow T_v = T - \frac{P - P_v}{\mu} \quad (7)$$

Substituting for the discharged molar flow rate ( $n_{out} = Q_g P_v / RT_v$ ) in Eqs. (1) and (2) leads to:

$$\frac{d}{dt}(\varepsilon_{eff}C) + \frac{dq}{dt} = \frac{-Q_g P_v}{RV_b \left( T - \frac{P - P_v}{\mu} \right)} \quad (8)$$

$$\begin{aligned} \frac{d}{dt} \left[ \left( \rho_g C_{pg} \varepsilon_{eff} + \rho_s C_{ps} (1 - \varepsilon_b) + C_{pl} \frac{qM_g}{1000} \right) T \right] \\ = H_{ads} \frac{dq}{dt} + \frac{q_A}{V_b} - \frac{Q_g P_v C_{pg} T^{M_g/1000}}{RV_b \left( T - \frac{P - P_v}{\mu} \right)} \end{aligned} \quad (9)$$

Differentiating Langmuir equation with respect to time provides:

$$\begin{aligned} \left[ (-\beta \gamma q_s P^{e^{\gamma/T}} / T^2 + \eta \theta b P T^{\eta-1}) \frac{dT}{dt} + b q_s \frac{dP}{dt} \right] (1 + bP) \\ \frac{dq}{dt} = \frac{- \left( -\beta \gamma P^{e^{\gamma/T}} T^2 \frac{dT}{dt} + b \frac{dP}{dt} \right) q_s b P}{(1 + bP)^2} \end{aligned} \quad (10)$$

Inserting Eqs. (10) into Eqs. (8) and (9) leads to:

$$\begin{aligned} \left[ \left( \varepsilon_t - \frac{q_s b P M_g}{1000 \rho_l (1 + bP)} \right) \left( \frac{-P}{RT^2 Z} \right) - \left( \frac{P M_g}{1000 \rho_l R T Z} - 1 \right) \right. \\ \left. \left( \frac{\eta \theta b P T^{\eta-1}}{1 + bP} + \frac{\beta \gamma q_s b P^2 e^{\gamma/T}}{T^2 (1 + bP)^2} - \frac{\beta \gamma q_s P e^{\gamma/T}}{T^2 (1 + bP)} \right) \right] \frac{dT}{dt} \\ + \left[ \left( \varepsilon_t - \frac{q_s b P M_g}{1000 \rho_l (1 + bP)} \right) \left( \frac{1}{RTZ} \right) - \left( \frac{P M_g}{1000 \rho_l R T Z} - 1 \right) \right. \\ \left. \left( \frac{q_s b}{1 + bP} - \frac{q_s b^2 P}{(1 + bP)^2} \right) \right] \frac{dP}{dt} = \frac{-Q_g P_v}{RV_b \left( T - \frac{P - P_v}{\mu} \right)} \end{aligned} \quad (11)$$

$$\begin{aligned} \left[ \rho_s C_{ps} (1 - \varepsilon_b) + \left( \frac{C_{pl} M_g T}{1000} - \frac{M_g^2 C_{pg} P}{10^6 \rho_l R Z} - H_{ads} \right) \right. \\ \left. \left( \frac{\eta \theta b P T^{\eta-1}}{1 + bP} + \frac{\beta \gamma q_s b P^2 e^{\gamma/T}}{T^2 (1 + bP)^2} - \frac{\beta \gamma q_s P e^{\gamma/T}}{T^2 (1 + bP)} \right) \right] \frac{dT}{dt} \end{aligned}$$

<sup>\*</sup>Total porosity could be also calculated using Eq. (16).

$$\begin{aligned}
 & + \left[ \left( \frac{M_g C_{pg} \epsilon_i}{1000 R_z} - \frac{M_g^2 C_{pg} q_s b P}{10^6 \rho_l R_z (1+bP)} \right) \right. \\
 & + \left. \left( \frac{C_{pl} M_g T}{1000} - \frac{M_g^2 C_{pg} P}{10^6 \rho_l R_z} - H_{ads} \right) \left( \frac{q_s b}{1+bP} - \frac{q_s b^2 P}{(1+bP)^2} \right) \right] \frac{dP}{dt} \\
 & = H_{ads} \frac{\partial q}{\partial t} + \frac{q_A}{V_b} - \frac{Q_g P_v C_{pg} T^{M_g} / 1000}{R V_b \left( T - \frac{P - P_v}{\mu} \right)} \quad (12)
 \end{aligned}$$

The natural convection heat transfer coefficient between cylindrical ANG storage system and its environment can be computed via the following equations [31]:

$$h = 1.42 \left( \frac{\Delta T}{L} \right)^{1/4} \quad \text{for vertical plane and cylinder} \quad (13)$$

$$h = 1.32 \left( \frac{\Delta T}{L} \right)^{1/4} \quad \text{for horizontal cylinder} \quad (14)$$

Now, Eqs. (10) to (12) should be solved simultaneously to provide all transient profiles of P, q, and T. Multivariate fourth-order Runge-

Kutta numerical method is used to deal with this task.

### DATA PREPROCESSING

As mentioned, three different case studies were used to demonstrate the reliable performances of our newly proposed lumped model. The Ridha et al. [16] experiment is the first case study which will be used to validate our model. They initially examined the methane adsorption capacity of two different types of activated carbons. Then the adsorbent which provided higher capacity of methane adsorption was selected for later experiments. Seven thermocouples inside a stainless steel chamber were used to measure the temperature of the bed at various radial and axial positions. Fig. 2(a) shows dynamic temperature variation at these locations. Two of these temperatures (T3, T4) practically measured the same values. Fig. 2(b) illustrates the time distribution of the spatial average temperatures of the above storage reservoir. This cumulative profile will be used to validate the proposed lumped model presented in the next section.

The second case study is borrowed from Mota et al. [2], who did not provide any experimental results and used a spatially distributed

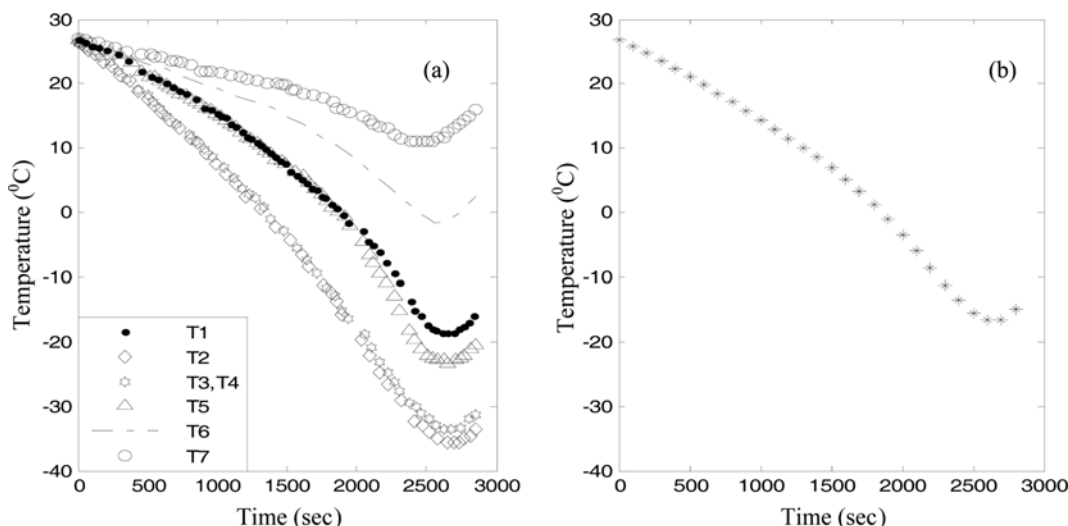


Fig. 2. (a) Experimental transient temperature profiles for AC-L/methane system borrowed from [16], (b) Computed average (bulk) temperature profiles.

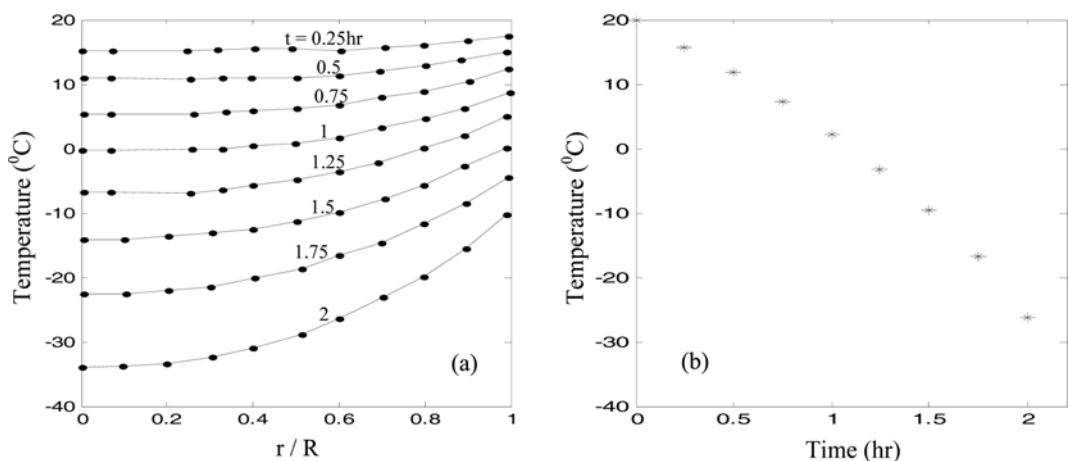


Fig. 3. (a) simulation transient radial temperature profiles of Mota et al. [2], (b) Spatially averaged bulk temperature profile.

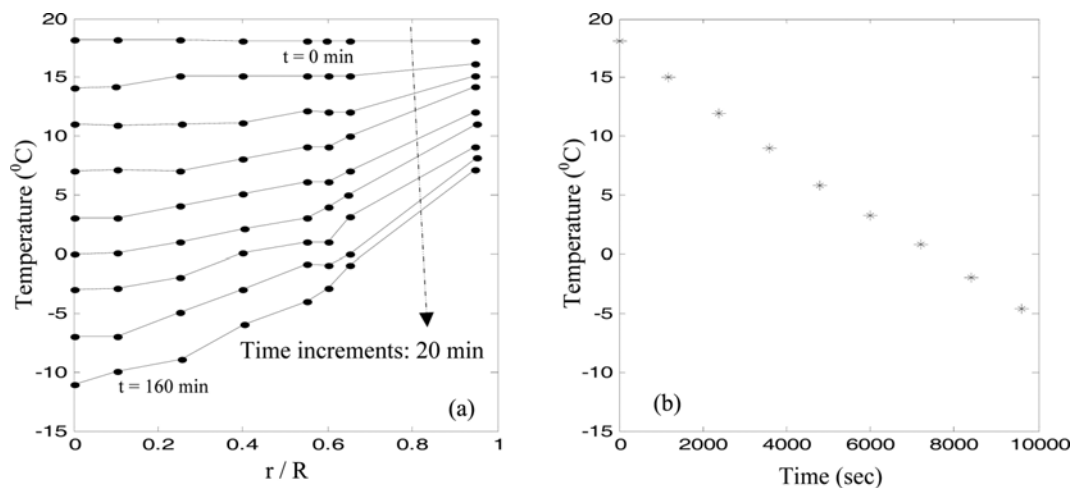


Fig. 4. (a) Experimental dynamic radial temperature distributions of Chang and Talu [1], (b) Corresponding transient averaged temperature profiles.

model to generate simulation data for two processes of dynamic fast adsorption and slow desorption of methane from natural gas stream over G216 activated carbon in a 50-liter horizontal cylinder. They assumed a pressure history to model the transient radial temperature distribution. Fig. 3(a) shows their two-hour predicted results for the slow discharge process. Once again, Fig. 3(b) provides the spatial average temperature distribution, which will be used later to validate our proposed model.

In the third attempt, the experimental data of Chang and Talu [25] for slow discharge of relatively pure methane (at the rate 6.7 // min, which was about one-quarter of the energy demand of a sub-compact car traveling at cruising speed) was used. The discharge process lasted about 2 hours and 40 minutes as shown in Figs. 4(a). The radial averaged bulk temperatures used for validation purposes are depicted in Fig. 4(b).

Data of Table (1) were used to solve ‘Equations 10 to 12’ and

Table 1. Required data set for simulation

	Ridha et al. [16]	Mota et al. [2]	Chang and Talu [1]
Type of data	Experimental-case # 1	Simulation-case # 2	Experimental-case # 3
<i>Activated carbon bed properties:</i>			
Type	Coconut shell	G216carbon pellets	N/A
Density	590 kg/m <sup>3</sup>	410 kg/m <sup>3</sup>	975 kg/m <sup>3</sup>
Pore volume	0.85 cm <sup>3</sup> /gr	N/A	N/A
Specific heat	650 J/kg K	650 J/kg K	1052 J/kg K
Effective porosity	0.8015	0.74	0.5
Assumed bulk porosity [32]	0.35	0.35	0.35
<i>Cylinder geometry:</i>			
Material	Stainless steel	Stainless steel	Carbon steel
Internal radius	0.035 m	0.14 m	0.1 m
Length	0.128 m	0.85 m	0.74 m
<i>Operational conditions:</i>			
Initial pressure	3.9 MPa	3.5 MPa	2.1 MPa
Depletion pressure	0.1 MPa	0.1013 MPa	0.166 MPa
Initial temperature	300 K	293 K	291 K
Ambient temperature	300 K	293 K	291 K
Flow rate	1 L/min	0.0185 Kg/min [18]	6.7 L/min
<i>Adsorption characteristics:</i>			
Heat of adsorption (–ΔH)	16e <sup>3</sup> J/mol [12]	17.6e <sup>3</sup> J/mol	(assumed as Mota et al.)
<i>Langmuir related parameters:</i>			
β	2.1210e <sup>-8</sup> [13]	1.0863e <sup>-7</sup>	2.4935e <sup>-8</sup>
γ	1.1879e <sup>3</sup> [13]	806	1.232e <sup>3</sup>
θ	3.7225e <sup>6</sup> [13]	1.7475e <sup>9</sup>	1.5654e <sup>6</sup>
η	-1.1290 [13]	-2.3	-1.015

compute the entire dynamic temperature, pressure and adsorbed amount distributions for various case studies borrowed from the literature [1,2,16]. Table 1 illustrates that different values were considered for the effective porosity of various adsorbents, while their bulk porosity is assumed to be the same. The average value of 0.35 for bulk porosity of the adsorbents was assumed based on the experimental data reported in reference [32]. The relations between bulk and total porosity could be updated from the following equations:

$$\varepsilon_p = \frac{V_p \times \rho_p}{1 - \varepsilon_b} \quad (15)$$

$$\varepsilon_t = \varepsilon_b + (1 - \varepsilon_b) \times \varepsilon_p \quad (16)$$

The computed results were then compared with above experimental and simulation data.

## SIMULATION RESULTS AND DISCUSSION

Three separate data of Table (1) were used to simulate the ANG vessel discharge processes under different operating conditions. Various simulation scenarios especially considering the effect of adsorbed phase heat accumulation are included. Some of these scenarios such as porosity variation during the discharge process have not been addressed previously. As mentioned earlier, three case studies and a recent simulation results reported by Hirata et al. [18] are used to validate our model predictions. For the sake of time and space saving, the selected results are presented for each case study under following scenarios:

1. Constant Langmuir parameters without adsorbed layer energy accumulation effect.
2. Variable Langmuir parameters without adsorbed layer energy accumulation effect.
3. Variable Langmuir parameters with adsorbed layer energy accumulation effect.
4. Variable Langmuir parameters, with adsorbed layer energy accumulation effect and considering porosity variation during discharge.

The first scenario would be the simplest and it is reasonable to expect that its prediction will be improved by each step with considering adsorbed phase effect, variation of Langmuir parameters and porosity variation during discharge.

As it will be demonstrated in the following examples (case studies), although all the considered parameters (variable Langmuir parameters, adsorbed layer energy accumulation effect, and porosity variation during discharge processes) have significant effect on the overall performance of the model predictions, the adsorbed layer energy accumulation effect is more pronounce than others.

### 1. First Case Study

To validate our proposed model, the first case study was selected from experimental data of Ridha et al.'s work [16]. Although the majority of data required for our model were available in the original article of Ridha et al. [16], some missing data are borrowed from other literatures for similar activated carbon [12,13]. Fig. 5 compares the obtained simulation results of the proposed lumped model in various scenarios with experimental data of Ridha et al. [16].

As can be observed, the improvement of the proposed model along

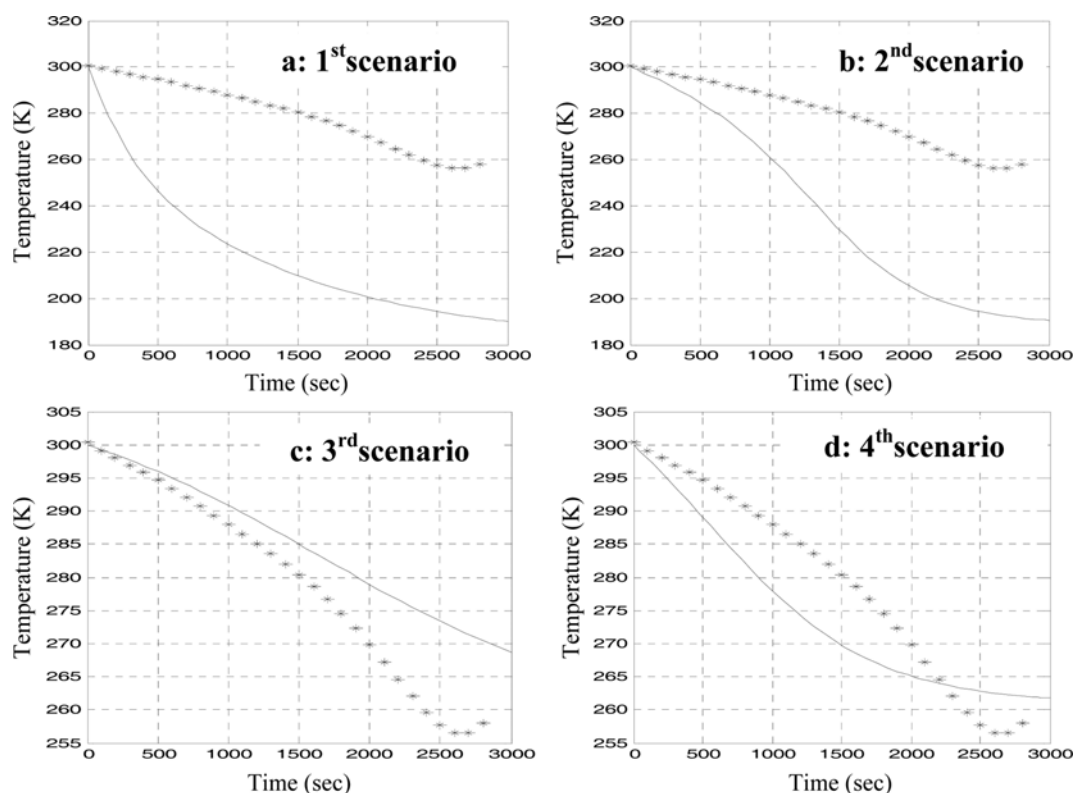


Fig. 5. Comparison of predicted temperature profiles (line) during discharge process and the experimental results of Ridha et al. (stars) for different scenarios.

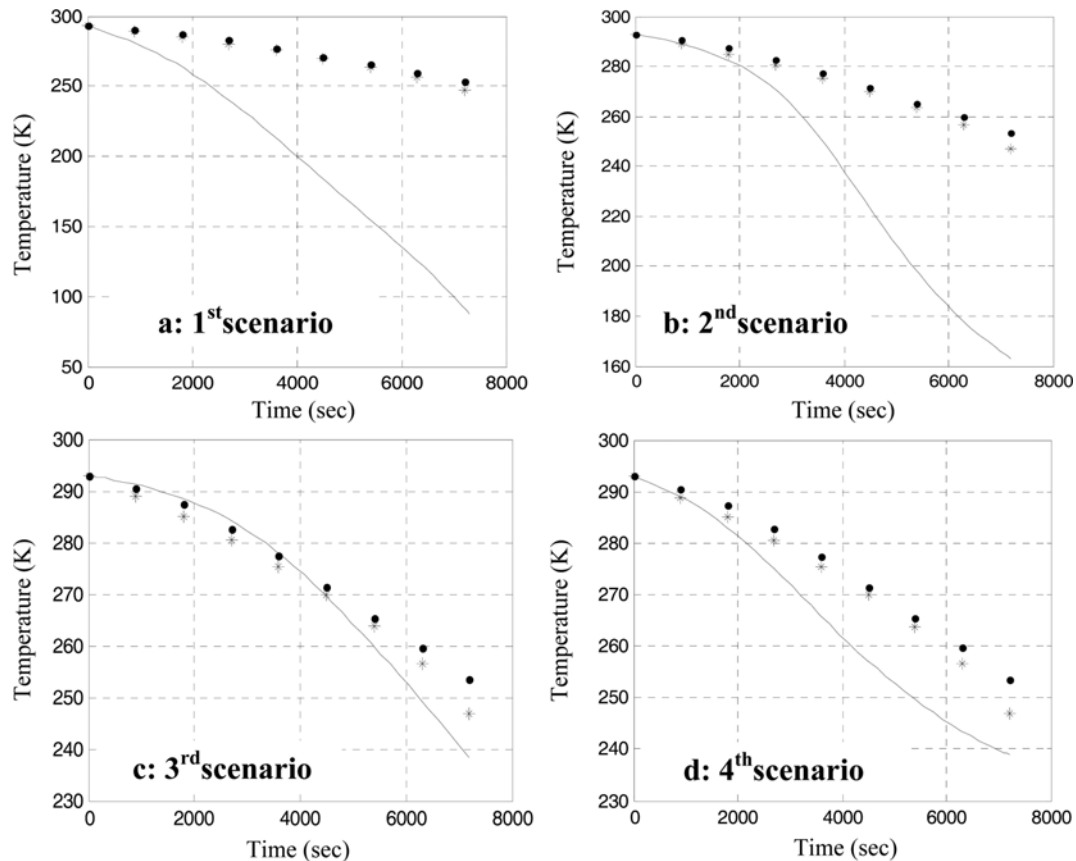


Fig. 6. Comparison of modeled temperature drop profiles during discharge (line), the result of Hirata et al. model [18] (circles), and work of Mota et al. [2] (stars) along mentioned scenarios.

four previously mentioned scenarios is quite impressive (especially for the three first scenarios). The combination of variable Langmuir parameters, adsorbed phase effect and porosity variation during discharge process has a profound effect on the overall performance of the proposed model. The latter has not been addressed previously.

The heat transfer supplied by the environment to ANG vessel during the discharge process tends to decrease the temperature drop rate. At some points, the temperature difference between the vessel and the environment is such that the heat transfer rate from the environment equals to the desorption heat required for discharge process. At this stage the vessel temperature should remain constant.

Otherwise, when the temperature difference between vessel and environment is sufficiently high, then the heat transfer from the ambient would be larger than the heat required for discharge process and therefore a temperature increase would be observed. So, the temperature increases could be due to the time variations of system properties or warming effect of ambient temperature.

## 2. Second Case Study

Simulation results provided by Mota et al. [2] were borrowed for as the second case study to validate our proposed lumped model. They simulated a typical ANG tank, especially emphasizing thermal effects and investigated various operational parameters on its performance. In 2009 Hitara et al. [18] used Mota et al.'s numerical results to validate their own mathematical model for slow discharge process from a methane storage tank. For comparison purposes and better validation of our lumped model, both predictions

of Hirata et al. and Mota et al. are included in this section. Fig. 6 illustrates a comparison of our simulation results for various scenarios with simulation data of Mota et al. and Hirata et al. averaged predictions. Although the distributed model presented by Hirata et al. [18] performs more adequately than our lumped model, our proposed model is much more convenient and provides very fast predictions with reasonable accuracy. It should be emphasized that the original data of Mota et al. was not produced experimentally and it was generated using a one dimensional (radial) model.

## 3. Third Case Study

The last validation experimental data set was borrowed from Chang and Talu [1]. The predictions of Hirata et al. [18] model are also included for better comparisons. A small error was observed in the reported results of Hirata et al. while using the time duration of Chang and Talu [1]. The original data of Chang and Talu were reported for every 20 minutes while Hirata et al. used the same data for every 15 minutes interval for up to 2 hours, as clearly mentioned in the caption of the corresponding figure. However, they mentioned that "The data was collected every 20 minutes for a 3 hours discharge process," which is clearly inconsistent with the caption of Fig. 5 of reference [18], suggesting a typo error in Figure caption.

Fig. 7 shows that our present lumped model predictions are much closer to the experimental data of Chang and Talu (especially when the combination effects of variable Langmuir parameters, adsorbed phase and porosity variation during discharge process are considered) compared to the simulation results of the relatively complex

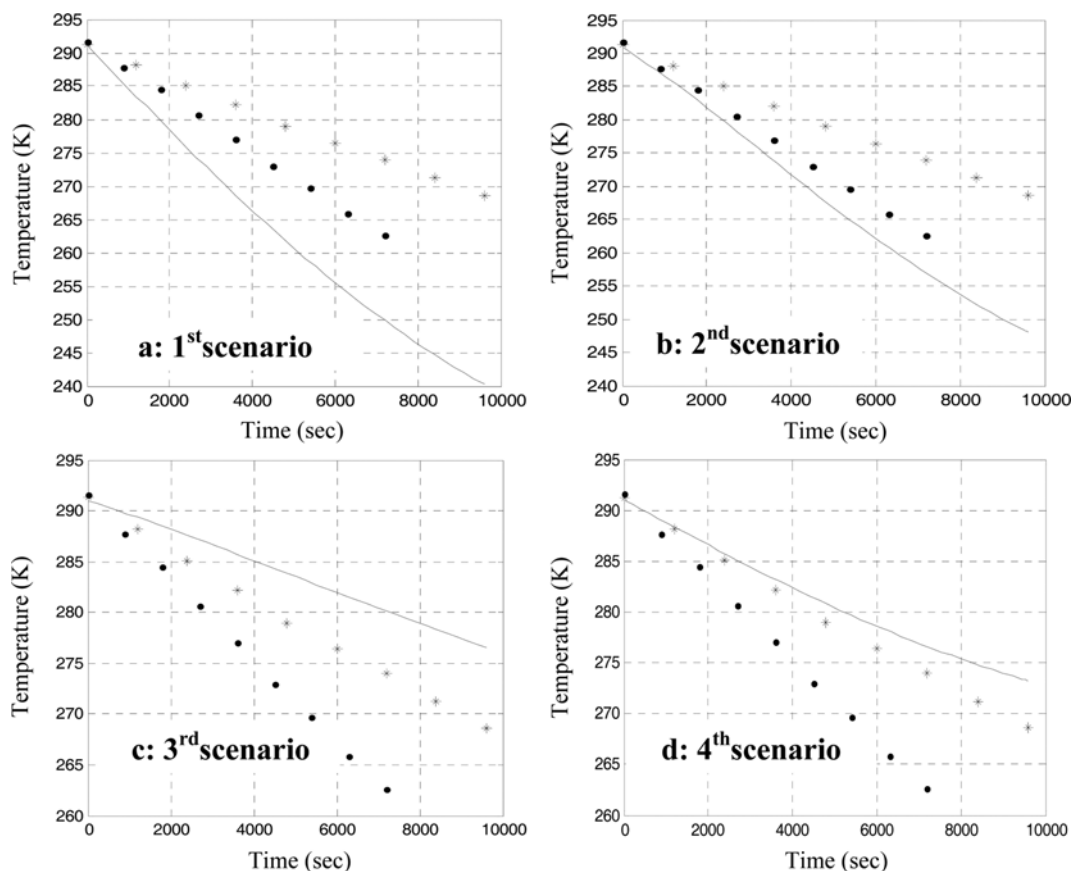


Fig. 7. Comparison of modeled temperature drop profiles during discharge (line), the result of Hirata et al. model [18] (circles), and experimental data of Chang and Talu [1] (stars) along mentioned scenarios.

model of Hirata et al. This issue emphasizes that our lumped model can be successfully employed for various cases while other presented models such as Hirata's model are case sensitive and can not be successfully applied for all cases.

### CONCLUSIONS

A convenient model based on lumped formulation was presented for reliable prediction of thermal behavior of ANG vessels during the discharge process. The model presents four different scenarios:

1. Constant Langmuir parameters without adsorbed layer energy accumulation effect.
2. Variable Langmuir parameters without adsorbed layer energy accumulation effect.
3. Variable Langmuir parameters with adsorbed layer energy accumulation effect.
4. Variable Langmuir parameters, with adsorbed layer energy accumulation effect and considering porosity variation during discharge.

It is clear that the latter scenarios have fewer simplifying assumptions and therefore are anticipated to provide more realistic predictions, as in the case of Chang and Talu data (third case study). At a first glance, the third scenario seems to provide better results for Ridha et al data. However, a closer examination of the results reveals that the fourth scenario leads to better correlation coefficients for all cases except Mota et al. data, as shown in Table 2. Note that the

Table 2. Computed correlation coefficient values for all case studies

	Correlation coefficient value		
	Ridha et al.	Mota et al.	Chang and Talu
1 <sup>st</sup> Scenario	-16.8167	-36.3835	-6.5756
2 <sup>nd</sup> Scenario	-10.712	-11.2644	-2.5673
3 <sup>rd</sup> Scenario	0.6967	0.9012	0.4533
4 <sup>th</sup> Scenario	0.7948	0.6008	0.8788

Mota data are synthetic results while other data are experimental measurements.

Figs. 5 to 7 clearly demonstrate that the proposed lumped model performs very adequately on prediction of all transient temperature profiles during discharge processes of various real and simulation case studies provided that proper assumptions are applied. Various scenarios such as variation of Langmuir parameters with temperature, effect of the adsorbed phase, and the porosity variation were considered. It was also shown that relaxing all those assumptions has significant improvement on the simulation results. Also, the proposed model provided very satisfactory predictions when experimental data were used for validation purposes.

### NOMENCLATURE

A : surface area of ANG tank [ $\text{m}^3$ ]

$b$	: Langmuir parameter [ $\text{Pa}^{-1}$ ]
$C_{pg}$	: gas heat capacity [ $\text{J/Kg K}$ ]
$C_{pl}$	: adsorbate heat capacity [ $\text{J/Kg K}$ ]
$C_s$	: adsorbent heat capacity [ $\text{J/Kg K}$ ]
$C$	: gas concentration [ $\text{mol/m}^3$ ]
$H_{ads}$	: heat of adsorption [ $\text{J/mol}$ ]
$H_{out}$	: enthalpy [ $\text{J}$ ]
$h$	: heat transfer coefficient [ $\text{W/K m}^2$ ]
$M_g$	: molecular weight of gas
$n$	: molar flow rate [ $\text{mole/s}$ ]
$P$	: pressure of bed [ $\text{Pa}$ ]
$P_v$	: pressure after valve [ $\text{Pa}$ ]
$q$	: adsorbed amount [ $\text{mol/m}^3 \text{ bed}$ ]
$q_s$	: Langmuir parameter [ $\text{mol/m}^3 \text{ bed}$ ]
$q_A$	: heat loss [ $\text{J/s}$ ]
$Q$	: discharge flow rate [ $\text{m}^3/\text{s}$ ]
$R$	: universal gas constant [ $\text{J/mol} \cdot \text{K}$ ]
$T$	: temperature of bed [ $\text{K}$ ]
$T_v$	: temperature after valve [ $\text{K}$ ]
$t$	: time [ $\text{s}$ ]
$V_b$	: bed volume [ $\text{m}^3$ ]
$V_p$	: pore volume [ $\text{cm}^3/\text{gr}$ ]
$z$	: compressibility factor

### Greek Symbols

$\beta$	: constant of Eq. (4) [ $\text{Pa}^{-1}$ ]
$\gamma$	: constant of Eq. (4) [ $\text{K}$ ]
$\theta$	: constant of Eq. (5) [ $\text{mol/m}^3 \text{ bed}$ ]
$\eta$	: constant of Eq. (5)
$\rho_b$	: bulk density [ $\text{gr/cm}^3$ ]
$\rho_l$	: adsorbed phase density [ $\text{Kg/m}^3$ ]
$\varepsilon_{eff}$	: effective porosity
$\varepsilon_b$	: bulk porosity
$\varepsilon_p$	: particle porosity
$\mu_A$	: Joule-Thomson coefficient [ $\text{Pa/K}$ ]

### REFERENCES

1. K. J. Chang and O. Talu, *Appl. Therm. Eng.*, **16**, 359 (1996).
2. J. P. B. Mota, A. E. Rodrigues, E. Saadatian and D. Tondeur, *Carbon*, **35**, 1259 (1997).
3. Z. Zhou, *Appl. Therm. Eng.*, **17**, 1099 (1997).
4. J. A. F. MacDonald and D. F. Quinn, *Fuel*, **77**, 61 (1998).
5. L. L. Vasiliev, L. E. Kanonchik, D. A. Mishkinis and M. I. Rabetsky, *Int. J. Therm. Sci.*, **39**, 1047 (2000).
6. K. Inomata, K. Kanazawa, Y. Urabe, H. Hosono and T. Araki, *Carbon*, **40**, 87 (2002).
7. J. P. B. Mota, I. A. A. C. Esteves and M. Rostam-Abadi, *Comput. Chem. Eng.*, **28**, 2421 (2004).
8. M. Bastos-Neto, A. Torres, D. Azevedo and C. Cavalcante, *Adsorpt.*, **11**, 147 (2005).
9. R. Basumatary, P. Dutta, M. Prasad and K. Srinivasan, *Carbon*, **43**, 541 (2005).
10. O. Pupier, V. Goetz and R. Fiscal, *Chem. Eng. Process.*, **44**, 71 (2005).
11. X. D. Yang, Q. R. Zheng, A. Z. Gu and X. S. Lu, *Appl. Therm. Eng.*, **25**, 591 (2005).
12. K. S. Walton, C. L. Cavalcante Jr. and M. D. LeVan, *J. Chem. Eng.*, **23**, 555 (2006).
13. D. C. S. Azevedo, J. C. S. Araújo, M. Bastos-Neto, A. E. B. Torres, E. F. Jaguaribe and C. L. Cavalcante, *Micropor. Mesopor. Mater.*, **100**, 361 (2007).
14. F. N. Ridha, R. M. Yunus, M. Rashid and A. F. Ismail, *Exp. Therm. Fluid. Sci.*, **32**, 14 (2007).
15. F. N. Ridha, R. M. Yunus, M. Rashid and A. F. Ismail, *Fuel Process. Technol.*, **88**, 349 (2007).
16. F. N. Ridha, R. M. Yunus, M. Rashid and A. F. Ismail, *Appl. Therm. Eng.*, **27**, 55 (2007).
17. H. Najibi, A. Chapoy and B. Tohidi, *Fuel*, **87**, 7 (2008).
18. S. C. Hirata, P. Couto, L. G. Lara and R. M. Cotta, *Int. J. Therm. Sci.*, **48**, 1176 (2009).
19. A. Sáez and M. Toledo, *Appl. Therm. Eng.*, **29**, 2617 (2009).
20. J. C. Santos, F. Marcondes and J. M. Gurgel, *Appl. Therm. Eng.*, **29**, 2365 (2009).
21. M. J. M. da Silva and L. A. Sphaier, *Appl. Energy*, **87**, 1572 (2010).
22. J. de Joode and Ö. Özdemir, *Energy Policy*, **38**, 5817 (2010).
23. W. Zhou, *Chem. Rec.*, **10**, 200 (2010).
24. J. M. Ejarque, *Energy Econ.*, **33**, 44 (2011).
25. D. S. Jurumenha and L. A. Sphaier, *Appl. Therm. Eng.*, **31**, 2458 (2011).
26. K. A. Rahman, W. S. Loh, A. Chakraborty, B. B. Saha, W. G. Chun and K. C. Ng, *Appl. Therm. Eng.*, **31**, 1630 (2011).
27. R. B. Rios, M. Bastos-Neto, M. R. Amora Jr., A. E. B. Torres, D. C. S. Azevedo and C. L. Cavalcante Jr., *Fuel*, **90**, 113 (2011).
28. R. P. Sacca Diaz and L. A. Sphaier, *Int. J. Therm. Sci.*, **50**, 599 (2011).
29. N. Kim, J. H. Lee, Y. S. Cho and W. Chun, *Energy*, **35**, 2717 (2010).
30. X. Lang, Sh. Fan and Y. Wang, *J. Nat. Gas. Chem.*, **19**, 203 (2010).
31. J. P. Holman, *Heat transfer*, Tenth Ed., McGraw Hill Higher Education, New York (2009).
32. J. S. Goodling, R. I. Vachon, W. S. Stelplflug, S. J. Ying and M. S. Khader, *Powder Technol.*, **35**, 23 (1983).